Vortex-lattice pinning in bulky single-phase $PbMo_6S_8$ and $SnMo_6S_8$ samples with various grain sizes

V. R. Karasik, E. V. Karyaev, V. M. Zakosarenko, M. O. Rikel, and V. I. Tsebro

P. N. Lebedev Physics Institute, USSR Academy of Sciences
(Submitted 21 April 1984)
Zh. Eksp. Teor. Fiz. **87**, 2114–2128 (December 1984)

Vortex lattice pinning is investigated in single-phase sintered bulk $PbMo_6S_8$ and $SnMo_6S_8$ samples with various (between 0.3 and 2.0 μm) average grain sizes. The sample compositions correspond to certain terminal points of the homogeneity region of the compounds. It is shown that the absolute values and forms of the dependences of the pinning force on the relative induction and on the temperature, $P_V(b,T)$, are significantly influenced by the grain size. The behavior of $P_V(b,T)$ is analyzed in conjunction with the measured vortex-lattice reversible response. It is shown that the principal pinning centers in the investigated samples are the grain boundaries. It follows from an analysis of the results that to increase appreciably the pinning force (the critical current density), especially in strong magnetic fields, it is necessary to strengthen the vortex pinning to the boundaries of the individual crystallites.

1. INTRODUCTION

Investigations of the critical currents in the ternary molybdenum sulfides (TMS) ($PbMo_6S_8$ and $SnMo_6S_8$, initiated by Alekseevskiĭ and co-workers[1–3] and continued by a number of others,[4–15] are of great interest and are quite timely: along with relatively high superconducting temperatures $T_c \lesssim 15$ K these compounds have record high upper critical magnetic fields $H_{c2} \lesssim 600$ kOe.

It is known that a nonzero nondissipative transport current can be made to flow through a type-II superconductor only if the latter has defects (pores, normal-phase inclusions, grain boundaries, dislocations, and others), which act as pinning centers for the vortex lines. The density of the critical current J_c is connected with the "volume" pinning force P_V by the relation $J_c B = P_V$ (B is the induction). This is the net force acting on a unit volume of the vortex lattice, and is the result of collective interaction of a large number of pinning centers with the vortex lattice. The value of P_V is determined, on the one hand, by the nature of the pinning forces (in other words, by the force f_p of the elementary interaction between an individual pinning center and the vortex lattice), and by their density N_p. On the other hand, it is determined by the elastic properties of the vortex lattice itself. The rigidity of the vortex lattice prevents an optimal arrangement of the pinning centers randomly distributed in the superconductor, and leads as a rule to a decrease of the total pinning force compared with its maximum value $P_V = N_p f_p$. Calculation of the volume pinning force P_V with allowance for the elastic properties of the vortex lattice, for a specific defect system (the problem of summing the elementary pinning forces f_p), is one of the most complicated problems of pinning theory, and there is at present no meeting of minds concerning many aspects of this problem (see, e.g., Refs. 16–20). This hinders the interpretation of the experimental results and makes it difficult to establish a connection between the observed values of P_V (or J_c) and the parameters of the microstructure of the superconducting material, especially when critical currents are investigated in samples having a rather complicated microstructure and in which the vortex lattice is pinned by defects of several types.

Measurements of the critical currents in ternary molybdenum sulfides were performed on samples that differ in form and in the method of sample preparation. The following were investigated: a) coatings produced on the surfaces of molybdenum foils or wires[1,4,12] by diffusion growth from the gas phase; b) bulky cylinders of compressed powders of the corresponding compound and annealed at high temperature[2,3,5,8]; c) thin films obtained by cathode sputtering of the initial components, followed by annealing[9–11]; d) wires prepared by cold drawing and subsequently heat treating metallic tubes (of Cu, Ag, Ta, Mo) filled with powdered material.[13–15] As a rule, higher values of J_c were observed in samples shown by x-ray diffraction analysis to contain, besides the principal rhombohedral TMS phase, also noticeable amounts of impurity phases, e.g., Mo and Pb in films of $Cu_x Mo_6S_8$ (Ref. 9) and $PbMo_6S_8$ (Ref. 10) or PbS, MoS_2, Pb and Mo in bulky samples of $Pb_{1.2}Mo_{6.4}S_8$ (Ref. 7). For lack of information on the dimensions and densities of the impurity-phase inclusions, it is impossible to estimate the effectiveness of these inclusions as pinning centers, the more so since high critical-current densities ($3 \cdot 10^8$ A/m^2 in a 10-T field at 4.2 K) were obtained in single-phase $PbMo_6S_8$ samples.[8] The effectiveness of other types of pinning center in the investigated TMS samples is just as uncertain. This, naturally, hinders the technology improvements needed to increase the current-carrying capacity of these superconducting materials. Considerable interest attaches therefore to an investigation of the critical currents in TMS samples having microstructure defects of a particular type.

We report here the results of investigations of vortex-lattice pinning in single-phase bulky sintered-powder samples of $PbMo_6S_8$ and $SnMo_6S_8$ in which the average grain size was varied (in the range 0.3–2.0 μm). The sample compositions corresponded to a definite limiting point of the homogeneity region of the given compound (see Refs. 21–23). This made it possible to carry out investigations on samples of one and the same composition with the same values (with-

 0038-5646/84/121221-08$04.00

in the limits of each series) of the principal superconducting parameters [T_c, $H_{c2}(T)$] and thereby facilitated greatly the comparison and analysis of the results.[24] The form of the functional interactions of the pinning point on the relative induction ($b = B/B_{c2}$) and temperature

$$P_v(b,\ T) \sim B_{c2}^n(T) f(b), \quad f(b) = P_v(b,\ T)/P_{v\,max}(T) \qquad (1)$$

was analyzed in conjunction with the data on the elastic properties of the vortex lattice and certain characteristics of the pinning centers, which were obtained by us in experiments on the reversible response of the vortex lattice to a weak alterating magnetic field.

2. SAMPLES

The single-phase $PbMo_6S_8$ and $SnMo_6S_8$ samples with different grain sizes were produced by a procedure similar to that described in Ref. 8. The samples were cylinders 5 mm in diameter and 12–15 mm long. The phase homogeneity was verified by x-ray structure and x-ray spectrum analysis. The average grain dimension was determined with a scanning electron microscope and ranged from 0.3 ± 0.1 to 1.3 ± 0.4 μm for $PbMo_6S_8$ and from 0.3 ± 0.1 to 2.0 ± 0.6 μm for $SnMo_6S_8$.

3. MEASUREMENT PROCEDURE

To measure the density of the critical current in bulky TMS samples we used inductive methods with weak trapezoidal[25,26] or sinusoidal[27] modulation of the magnetic field.

The general principle of the inductive methods of measuring J_c is the following. A sample in the form of a cylinder is placed in a constant magnetic field $H \gg H_{c1}$ parallel to an applied weak alternating $h(t)$. The alternating magnetic field penetrates into the sample to a depth $x(h)$ and alters the magnetic induction in a surface layer of cross section $\pi[R^2 - (R - x(h))^2]$ (R is the sample radius), which induces a voltage $V_S(t)$ in the coil wound around the sample. The relation between $x(h)$ and $V_S(t)$ is

$$x(h) = R[1 - (1 - V_S(t)/\mu_S V_n(t))^{1/2}], \qquad (2)$$

where $V_n(t)$ is the voltage induced in the receiving coil when the sample is in the normal state, and $\mu_S = (1/\mu_0)(dB/dH)$ is the magnetic permeability of the sample and is determined from the reversible $B(H)$ curve. For a type-II superconductor with a Ginzburg-Landau parameter $\varkappa \gg 1$ in fields $H \gg H_{c1}$ we have $\mu_S \approx 1$.

According to (2), the known value of $V_S(t)$ can be used to determine for any value of $h(t)$ the penetration depth $x(h)$, and to plot thereby the radial distribution of the magnetic induction in the sample. The gradient of this distribution gives the value of J_c at the corresponding distance from the sample surface.

Equation (2) is common to the all modulation procedures. The difference lies in the method of recording and interpreting the signal $V_S(t)$ induced in the receiving coil.

If the modulation is trapezoidal, the form of the response signal is analyzed on the linear-sweep segments $h(t) = a(t)$. At $x \ll R$ the induced voltage $V_S(t)$ is, as can be seen from (2), directly proportional to the penetration depth $x(h)$. Since the alternating magnetic field varies linearly with time, the $V_S(t)$ dependence constitutes the distribution of the magnetic induction inside the sample; the V_S axis corresponds then to the penetration depth x, and the t axis to the value of the magnetic induction.

In the case of sinusoidal modulation of the magnetic field the voltage $V_S(t)$ is measured by lock-in detection. The dc voltage S at the output of this detector is proportional to the integral of the input signal $V_S(t)$ over a time equal to half the period of the modulating field $h(t) = h_0 \sin(2\pi t/T)$, i.e.,

$$S = A \int_0^{T/2} V_S(t)\, dt,$$

where A is a constant that depends on the sensitivity of the apparatus. The synchronous detector is set to measure the signal that is in phase with the modulating field, and the measurement procedure consists of determining the values of S for different values of the amplitude h_0 of the modulating field. Relation (2) as applied to the sinusoidal modulation method is of the form

$$x(h_0) = R\left[1 - \left(1 - \frac{dS}{dh_0}\frac{1}{C}\right)^{1/2}\right], \qquad (3)$$

or, at $x(h_0) \ll R$,

$$x(h_0) = \frac{R}{2}\frac{dS}{dh_0}\frac{1}{C},$$

where $C = 2\pi R^2 A$. Consequently, given a plot of $S(h_0)$, the penetration depth $x(h_0)$ can be calculated from the derivative dS/dh_0.

The sinusoidal modulation method has high sensitivity and was used by us to investigate the response of a vortex lattice to an alternating magnetic field of very low amplitude, when the forces resulting from the periodic variation of the induction on the sample surface can produce only small oscillations of the vortex filaments about the equilibrium position. The displacements of the vortices and the corresponding variation of the magnetic flux in the sample have in this case no hystersis (are reversible).[27–30]

The experimental setup, a block diagram of which is shown in Fig. 1, is described in detail in Refs. 24 and 31. The sample was placed in a constant magnetic field of a superconducting solenoid capable of producing fields of intensity up to 165 kOe. The alternating magnetic field of frequency from 10 to 100 Hz and amplitude up to 500 Oe was produced by flow of alternating current through a modulating coil made of very pure aluminum wire with a resistance ratio $R_{300\,K}/R_{4.2\,K} > 10^4$. This has made it possible to reduce to a minimum the heat released from its turns in the case of large ac current flow (up to 40 A) and by the same token perform the measurements in a wide range of intermediate temperatures.

The $V_S(t)$ signal induced in the receiving coil was amplified and recorded with a high-sensitivity lock-in detector (in the case of sinusoidal modulation of the magnetic field), or else recorded with a stroboscopic integrator connected to an x-y plotter (in the trapezoidal-modulation method).

The parasitic signal due to variation of the magnetic

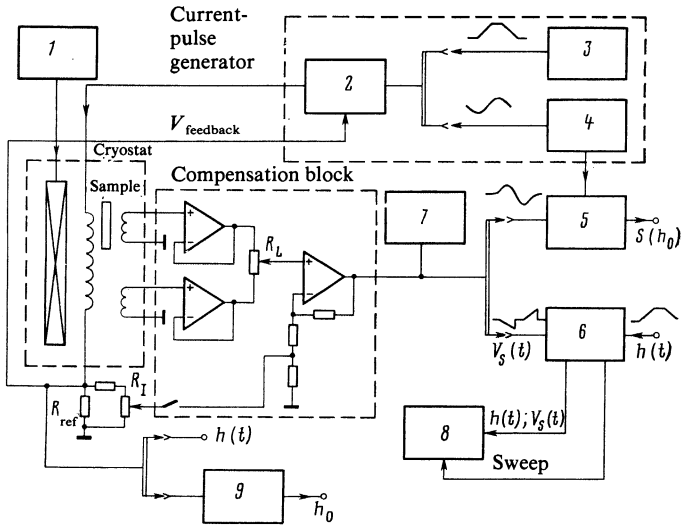

FIG. 1. Block diagram of experimental setup. 1—current source, 2—power amplifier, 3—trapezoidal-pulse generator, 4—GZ-102 acoustic-frequency generator, 5—PAR-120 lock-in detector, 60 PAR-162 stroboscopic integrator, 7—oscilloscope, 8—automatic x-y plotter, 9—V2-28 voltmeter.

field in the space between the sample surface and the turns of the receiving coil was cancelled out in part by a signal (adjusted by potentiometer R_L) induced in the compensating coil. At sinusoidal modulation, for a higher degree of compensation, a voltage from potentiometer R_I is used. This voltage is in phase with the current flowing in the modulation coil and with the field $h(t)$.

4. EXPERIMENTAL RESULTS

a) Critical-current density and pinning force

Figure 2 shows the field dependences, measured by the trapezoidal-modulation method, of the densities of the critical currents of samples $PbMo_5O_8$ and $SnMo_6S_8$ with varying grain sizes. It can be seen that decreasing the average grain size of either sample increases the critical current substantially. This alters the character of the $J_c(B)$ dependence. This takes place primarily at magnetic fields up to 6–8 T; in strong magnetic fields ($B > 10$ T) the change of the microstructure has a significantly smaller effect on J_c.

Figures 3 and 4 illustrate the changes of the $P_V(b)$ curves with change of temperature for samples with different grain sizes. The exponent of $B_{c2}(T)$ in the expression for the pinning force [see (1)] can be estimated from the data of Fig. 5, where a log-log plot of $P_V(b = 0.2)$ vs the upper critical field B_{c2} at the corresponding temperature is shown.

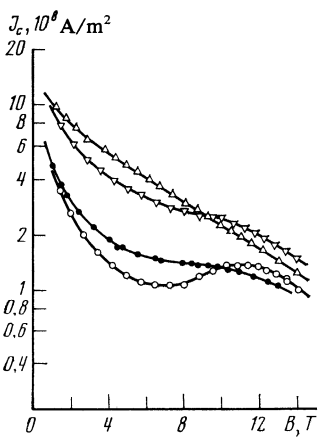

FIG. 2. Critical current density vs magnetic field at $T = 4.2$ K for $PbMo_6S_8$ samples with grain size: △—0.3 ± 0.1 μm and ●—1.3 ± 0.4 μm, and for $SnMo_6S_8$ samples with grain size: ▽—0.3 ± 0.1 μm and ○—2.0 ± 0.6 μm.

For $PbMo_6S_8$ samples with grain size $d \approx 0.3$ μm the experimental points of $P_V(b)|_{T=\text{const}}$ are described by a universal (temperature-independent) power law $f(b) = b^{1/2}(1-b)^2$, whereas for the temperature-independent part we have $P_V(T) \sim B_{c2}^{5/2}(T)$, i.e., the pinning force satisfies a scaling law of the form

$$P_V(b, T) \sim B_{c2}^{5/2}(T)\, b^{1/2}(1-b)^2.$$

For $PbMo_6S_8$ with 0.7 μm grains the plots of $P_V(b)$ at various temperatures are similar in form, but at large b the experimental points lie somewhat above the $f(b) = b^{1/2}(1-b)^2$ curve, and furthermore $P_V(T) \sim B_{c2}^2(T)$. Finally, the scaling law does not hold for samples with average grain size 1.3 μm. The form of the $P_V(b)$ curves depends strongly on temperature; an additional maximum appears and its position shifts towards larger b with rising temperature.

In the case of $SnMo_6S_8$ there is no scaling law for $P_V(b, T)$ for any of the investigated samples with d from 0.3 to 2.0 μm. In the samples with ≈ 0.3 μm grain the $P_V(b)$ curves are already close in shape to the $P_V(b)$ plots of the $PbMo_6S_8$ curves with $d \approx 1.3$ μm, except that the additional maximum at $b \gtrsim 0.5$ is more strongly pronounced. Despite the complicated form of the $P_V(b)$ curves for the $SnMo_6S_8$ samples, the decrease of the pinning force at large b obeys the same law $b^{1/2}(1-b)^2$. This circumstance is illustrated in Fig. 6, where the data obtained at $T = 7.0$ K for $SnMo_6S_8$ samples with different grain sizes are plotted with P_V and $b^{1/2}(1-b)^2$ as coordinates.

It was noted above that a change of the microstructure affects less the critical-current density in strong magnetic fields than in weak ones. This is clearly seen from a comparison of the corresponding $P_V(b)$ curves. Thus, Fig. 7 shows plots of $P_V(b)$ at $T = 7.0$ K for $PbMo_6S_8$ and $SnMo_6S_8$ samples with different grain sizes. An increase of the pinning force with decreasing d takes place at $b \lesssim 0.5$, whereas at large b the pinning force changes insignificantly and follows,

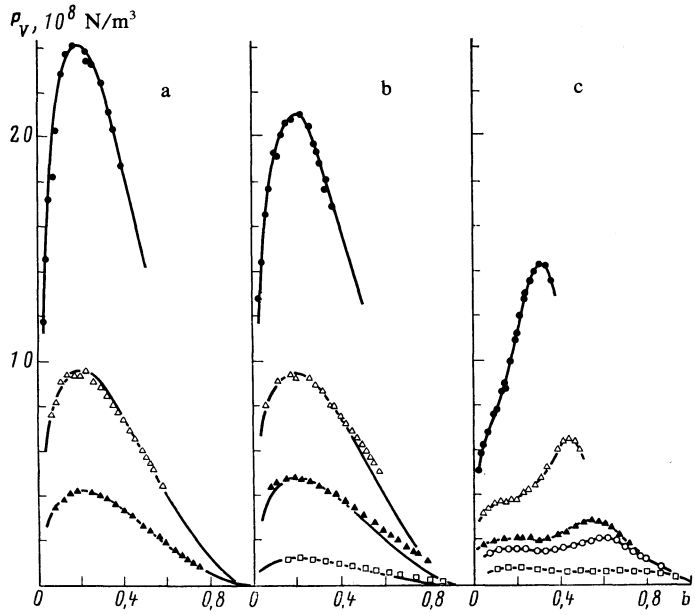

FIG. 3. Pinning force vs relative induction at various temperatures: ●—4.2 K; ▲—8.5 K; ○—9.0 K; □—10.5 K for $PbMo_6S_8$ samples with grain size $0.3 \pm 0.1\,\mu$m (a), $0.7 \pm 0.2\,\mu$m (b) and $1.3 \pm 0.4\,\mu$m (c). The solid lines in Figs. a and b are plots of $P_V(b) \sim b^{1/2}(1-b)^2$.

independently of the grain size and of the type of compound, a single quadratic law $P_V(b) \sim (1-b)^2$.

b) Investigation of reversible response of vortex lattice

As already noted, sinusoidal modulation of the magnetic field permits a study of phenomena connected with reversible displacements of a vortex lattice under the influence of a weak magnetic field. In this method, the first data to be reduced are the dependences of the lock-in-detector signal S on the amplitude b_0 of the modulating field [see Eq. (3)]. By way of example, Fig. 8 shows plots of $S(b_0)$ for the $SnMo_6S_8$ sample with grain size $d \approx 0.3\,\mu$m, while Fig. 9 shows the plots, obtained by differentiating the $S(b_0)$ curves, of the ac field penetration $x(b_0)$ as a function of the field amplitude.[1)] These data establish the character of the variation of the average restoring force F exerted on the vortices by the pinning centers as a function of the displacement u of the vortices from the equilibrium position, since (see Ref. 18)

$$F(u_0) = \frac{1}{\mu_0}\frac{b_0\,db_0}{dS} B_0 \cdot 2A\pi R, \quad u_0 = \frac{S(b_0)}{2\pi R b_0 A},$$

where u_0 is the displacement of the vortices at the sample surface, and B_0 is the induction.

Figure 10 shows plots of $F(u_0)/BJ_c$ for $PbMo_6S_8$ and $SnMo_6S_8$ samples with grain size $0.3\,\mu$m. It can be seen that at sufficiently small u_0 the restoring force is directly proportional to the displacement of the vortices from the equilibrium position, $F(u_0) \sim ku_0$. With increasing u_0, the value of $F(u_0)$ approaches its limit BJ_c, and the vortical lattice goes over into the critical state. The region of the reversible displacements of the vortex filaments is customarily characterized by a parameter d_0 called the "interaction length." From

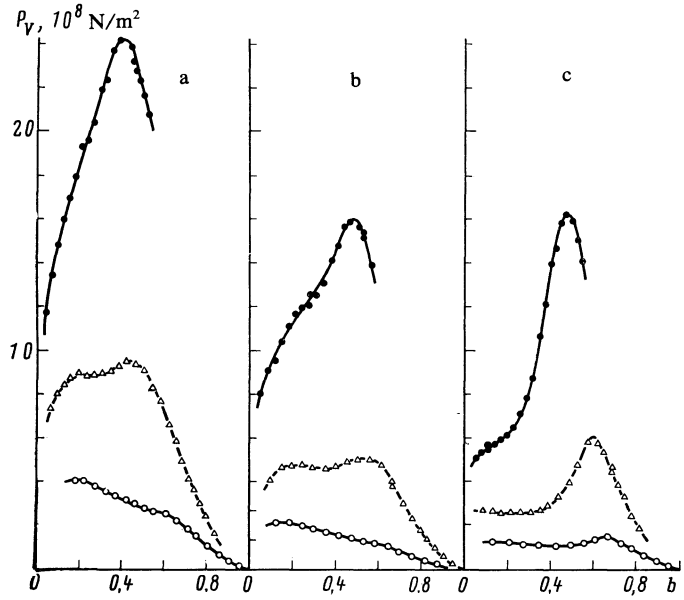

FIG. 4. Pinning forces vs relative induction at various temperatures: ●—4.2 K; △—7.0 K; ○—9.0 K for $SnMo_6S_8$ with grain size $0.3 \pm 0.1\,\mu$m (a), $1.0 \pm 0.3\,\mu$m, and $2.0 \pm 0.6\,\mu$m (c).

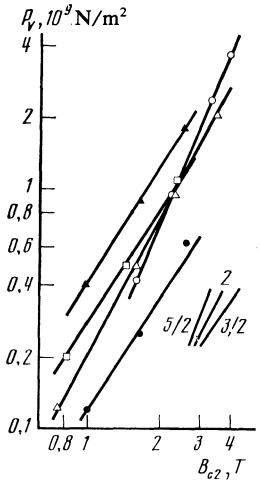

FIG. 5. Log-log plots of pinning force at $b = 0.2$ vs B_{c2} at the corresponding temperatures for $PbMo_6S_8$ with grain size: ○—0.3 ± 0.1 μm and △—0.7 ± 0.2 μm and $SnMo_6S_8$ samples with grain size: ▲—0.3 ± 0.1 μm, □—1.0 ± 0.3 μm, ●—2.0 ± 0.6 μm.

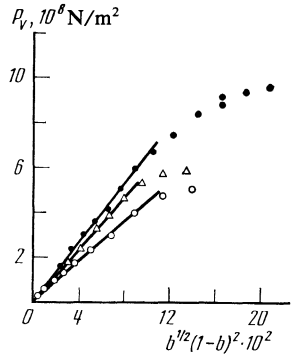

FIG. 6. Pinning force vs $b^{1/2}(1-b)^2$ at $T = 7.0$ K for $SnMo_6S_8$ samples with grain size: ●—0.3 ± 0.1 μm, ○—1.0 ± 0.3 μm, △—2.0 ± 0.6 μm.

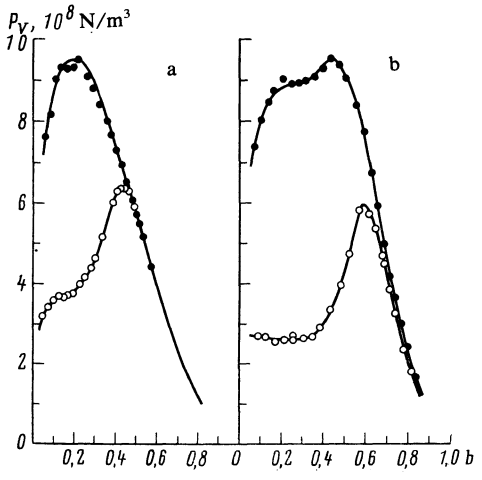

FIG. 7. Pinning force vs relative induction at $T = 7.0$ K for $PbMo_6S_8$ samples (a) with grain size: ●—0.3 ± 0.1 μm and ○—1.3 ± 0.4 μm, and for $SnMo_6S_8$ samples with grain size: ●—0.3 ± 0.1 μm and ○—2.0 ± 0.6 μm.

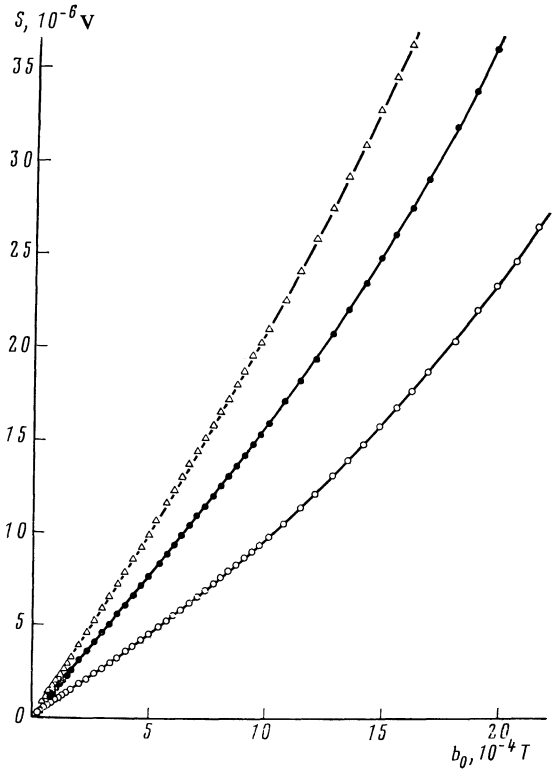

FIG. 8. Output signal S of lock-in detector vs amplitude of modulating field for $SnMo_6S_8$ sample with grain size 0.3 ± 0.1 μm at $T = 4.2$ K in magnetic fields: ○—6.08 T, ●—8.47 T, △—11.0 T.

d_0 we can estimate the distance by which the vortex filaments must be displaced from the equilibrium position in order to reach the critical value of the restoring force $F(u)$ (the pinning force). Thus for $PbMo_6S_8$ (see Fig. 10) at $B = 10.5$ T and $T = 4.2$ K we have $d_0 \approx 3$ Å.[2)]

In the region of reversible displacements of the vortices from the equilibrium positions, any change of the induction on the sample surface, as well as the associated changes of the vortex-lattice deformation, is exponentially damped, as shown in Ref. 30, at a certain depth λ_0^*, so that at a distance $x > \lambda_0^*$ the vortex lattice remains undeformed compared with its initial state. The damping of the deformations is due to the screening action of the pinning centers, which hinder

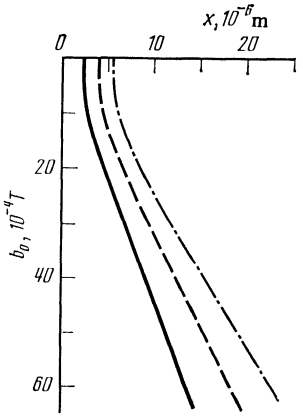

FIG. 9. Plots of penetration depth x vs alternating field amplitude b_0 for $SnMo_6S_8$ sample, obtained by differentiating the $S(b_0)$ plots of Fig. 8.

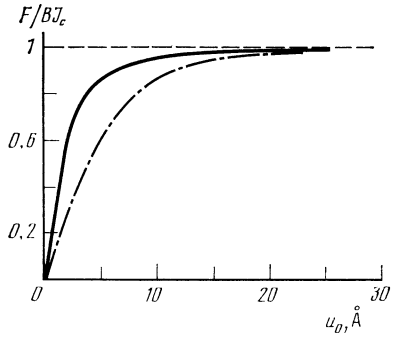

FIG. 10. Restoring force vs displacement of vortice from equilibrium position for $SnMo_6S_8$ samples (dash-dot line) in a magnetic field 11 T and for $PbMo_6S_8$ samples (solid line) in a field 10.15 T, with grain size 0.3 ± 0.1 μm, at 4.2 K.

the deviations of the vortices from the equilibrium positions. In the general case λ_0^* depends both on the elastic properties of the vortex lattice and on the physical nature and structure of the system of pinning centers in the investigated samples. The values of λ_0^* are determined in experiment from the initial section of the $x(b_0)$ curve (see Fig. 9), where $x(b_0) \approx \text{const} \equiv \lambda_0^*$.

Figure 11 shows the values of λ_0^* and d_0 at $T = 4.2$ K as functions of the relative induction b for $PbMo_6S_8$ and $SnMo_6S_8$ samples with grain size 3 μm. The interaction length for the $PbMo_6S_8$ sample decreases smoothly with increasing b, whereas for $SnMo_6S_8$ the $d_0(b)$ plot is nonmonotonic with a maximum in the region $b \approx 0.45$. The decrease of d_0 in this sample at $b \gtrsim 0.5$ is accompanied also by a decrease of the penetration depth λ_0^*. It must be noted that the maximum value of d_0 is observed in the same range of the relative induction as the maximum on the $P_V(b)$ curve [see Fig. 4(a)].

5. DISCUSSION

Let us analyze in greater detail the $P_V(b,T)$ dependences for $PbMo_6S_8$ and $SnMo_6S_8$ samples with various grain sizes, in conjunction with the reversible-response data $\lambda_0^*(b)$ and $d_0(b)$ that characterize the elastic displacements of the vortex filaments from the pinning centers. It is of interest first of all

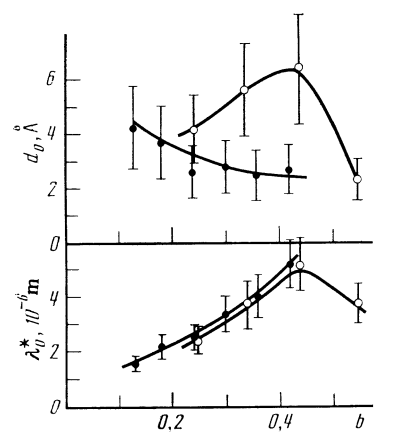

FIG. 11. Dependence of the parameters λ_0^* and d_0 of the reversible response of a vortex lattice on the relative induction for the samples: ●—$PbMo_6S_8$, ○—$SnMo_6S_8$ with grain size 0.3 ± 0.1 μm at $T = 4.2$ K.

to compare the available experimental material with the result of the theoretical papers,[20,32–35] where an attempt was made to determine, within the framework of a new statistical approach, the volume pinning force $P_V(b,T)$ for different categories of pinning centers. The theory[20,32–35] was based on data concerning the character of propagation of elastic strains in a vortex lattice[27,30,36,37] and on the collective-pinning concept developed by Larkin and Ovchinnikov.[38,39] According to the latter, the presence of pinning centers disturbs the long-range order of the arrangement of the vortex filaments, and the vortex lattice must be regarded as an assembly of individual regions V_c (correlation volumes), within the limits of which the short range order is preserved and which can be displaced relative to one another by a distance $\lesssim \xi$ under the influence of external forces (here ξ is the coherence length). In the statistical summation of the elementary forces f_p and in the calculation of P_V the authors of Refs. 20 and 32–35 determined the force exerted by the pinning centers on each of the separated volumes V_C, under the condition that the remaining lattice action V_c by an elastic force characterized by the modulus α. It is significant that the parameter α introduced into the theory depends on the defect density and on the elementary pinning forces, so that the approach constitutes essentially of a self-consistent determination of α and p_V.

When N_p and f_p are different, the correlation volume also varies in a wide range. Thus for example, at not too large N_p ($N_p \leqslant 1/a_f^3$, where a_f is the distance between the vortices), V_C increases with decreasing f_p, from $V_C \approx d_p^3$ (which is valid for pinning centers that break down the vortex lattice to the "liquid" state) to $V_C = V \gg d_p^3$ (at smaller f_p, when the "lattice" approximation is valid). Depending on the ratio $N = V_C/d_p^3$, the system of pinning centers in the superconductor pertains to "dense" ($N \gg 1$) or "dilute" ($N \approx 1$) limits. Let us estimate the value of N in the investigated $PbMo_6S_8$ and $SnMo_6S_8$ samples with grain size $d \approx 0.3$ μm. According to Ref. 20, $V_C \approx (\lambda_0^*)^2 \cdot 2a_f$ so that by putting $d_p = d \approx 0.3$ μm we obtain for the $PnMo_6S_8$ sample $N \geqslant 10$ already at $b \gtrsim 0.25$, and the criterion of a dense system of pinning centers is satisfied in these samples.

For the force P_V of pinning on a dense system of centers, Refs. 33–35 predict a quadratic relation $P_V(b) \sim (1-b)^2$ at large b in those cases when the f_p of the given centers is insufficient to break down the vortex lattice to the "liquid" state. In terms of the elastic modulus α, the range of f_p in which the $P_V(b) \sim (1-b)^2$ relation holds is determined by the inequality $\alpha(f_p) \lesssim \sqrt{3}C_{66}/2\pi$ (where C_{66} is the shear modulus of the vortex lattice), since in the lattice approximation $\alpha(f_p)$ increases with increasing f_p and reaches saturation at the level $\approx \sqrt{3}C_{66}/2\pi$. The elastic modulus α can be determined from the known value of λ_0^* by using the relation (see Ref. 16)

$$\alpha = B\Phi_0/\mu_0(\lambda_0^*)^2,$$

where Φ_0 is the magnetic-flux quantum.

Figure 12 shows the $\alpha(b)$ plots for the investigated $PbMo_6S_8$ and $SnMo_6S_8$ samples with $d \approx 0.3$ μm. The same figure shows the values of $C_{66}(b)$ calculated from the formula

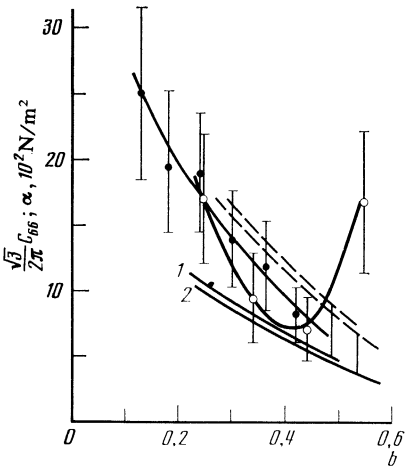

FIG. 12. Elastic modulus α vs relative induction for the samples: ●—$PbMo_6S_8$, ○—$SnMo_6S_8$ with grain size 0.3 ± 0.1 μm at $T = 4.2$ K. The solid lines show plots of $C_{66}(b)$ for $PbMo_6S_8$ (curve 1) and $SnMo_6S_8$ (curve 2) at $\varkappa$ equal, respectively, to 135 and 100; the dashed lines show the same dependence for $\varkappa = 100$ and 75.

$$C_{66}=0.13\mu_0 H_{c2}^2(1-b)^2\varkappa^{-2},$$

which is known to be valid at not too small b. The Ginzburg-Landau parameter $\varkappa$ was estimated from the formula

$$\varkappa^2=1.27\cdot 10^3\rho_0 dH_{c2}/dT,$$

obtained from the Gor'kov equation for $\varkappa$ and the known relation for the heat-capacity jump in the BCS theory.

For the $PbMo_6S_8$ and $MnMo_6S_8$ samples investigated by us, the values of dH_{c2}/dT measured (by determining the end point of the superconducting transition) are 44 and 33 kOe/K, and the remaining resistivities are respectively $2.9\cdot 10^{-4}$ and $1.4\cdot 10^{-4}$ $\Omega\cdot$ cm. This yields values $\varkappa\approx 130$ for $PbMo_6S_8$ and $\varkappa\approx 100$ for $SnMo_6S_8$. To show the extent to which the inaccuracy of influences the quantity $C_{66}\sim\varkappa^{-2}$, the dashed lines in the same Fig. 12 show the values of C_{66} for $PbMo_6S_8$ at $\varkappa = 100$ and $SnMo_6S_8$ at $\varkappa = 75$.

As can be seen from the data shown in Fig. 12, for the samples of both systems the values of $\alpha(b)$ agree within the limits of the measurement and estimate errors with $(\sqrt{3}/2\pi)C_{66}$. This classifies the pinning centers in the investigated samples, in terms of f_p, as relatively weak and as not causing breakdown of the vortex lattice to the liquid state.

Thus, the data obtained on the system of pinning centers (relatively small f_p, "dense" limit) and the results of Refs. 33–35 corroborate the form of the functional relation $P_V(b)\sim(1-b)^2$ observed in the $PbMo_6S_8$ and $SnbMo_6S_8$ samples (see Figs. 3 and 6) in strong magnetic fields.

The theory[20,33] explains also the weak dependence of P_V on the average grain size at large b (see Fig. 7). Indeed, the fact that the modulus α reaches in our samples the limit $(\sqrt{3}/2\pi)C_{66}$ of the "lattice" approximation means that increasing the density of the pinning centers without changing f_p cannot increase substantially α and hence the volume pinning force $P_V = Ba d_0/\Phi_0$. The reason is that the increase in the number of centers decreases simultaneously the effective action of each center on the vortex lattice. The decrease of the effectiveness of an individual pinning center is due to the screening action of the center, which restrict the size of the instability region of the given pinning center.

In all the $SnMo_6S_8$ samples investigated by us, as well as in the $PbMo_6S_8$ samples with $d\approx 1.3$ μm, the regions where the pinning force is quadratic in the relative induction precede the supplementary maximum of $P_V(b)$, and a nonmonotonic character of $d_0(b)$ is observed (see Fig. 11), with a maximum at the same values of b. At $b = 0.45$ the value of d_0 for the $SnMo_6S_8$ sample is ≈ 6 Å, or double the corresponding value for [3)] $PbMo_6S_8$. Since d_0 provides an estimate of the average distance to which the vortex filaments must be displaced from the equilibrium to reach the critical pinning force, the anomalous increase of P_V in strong magnetic fields is apparently due to the considerable displacements, and hence to the more favorable arrangement of definite parts of the vortex lattice relative to the pinning center. The "attunement" of the vortex lattice to the arrangement of the pinning centers, which constitutes an increase of the number of pinning centers that are simultaneously in contact with the vortex lattice, is called the "synchronization effect."

Synchronous pinning (see Ref. 16) is most probable in the case when the vortex lattice becomes attached to a system of planar (or linear) defects separated by rather large distances. It was indicated for this case (see also Refs. 40–43) that an important role in the synchronization effect is played apparently by the defects of the vortex lattice itself, whose rigidity is thereby decreased. It should be noted that the influence of the vortex-lattice defects (e.g., dislocations) on the onset of the synchronized state depends on the density of the pinning centers in the sample. Thus, in samples with larger N_p the dislocation climb effects will be hindered by the interaction of the dislocations with the pinning centers.

As noted in Ref. 20, the onset of the synchronized state should be accompanied by a decrease of the depth of penetration λ_0^*, a fact that reflects the weakening of the correlations between the pinning centers, and by a corresponding increase of the elastic modulus α. These features (the decrease of λ_0^*, the preceding growth of $d_0(b)$, as well as the more pronounced manifestation of the anomalous maximum of $P_V(b)$ for samples with lower grain-boundary density) manifest themselves distinctly in the samples investigated by us. There is therefore every reason for assuming that the complicated character of the $P_V(b)$ dependences in the $SnMo_6S_8$ samples, as well as in $PbMo_6S_8$ samples with $d\approx 1.3$ μm, is due to the synchronization effect. It must be noted in this connection that the synchronization effect, as shown by a comparative analysis of the $P_V(b)$ curves (see Figs. 3 and 4) for $PbMo_6S_8$ and $SnMo_6S_8$ samples with identical grain size, manifests itself more strongly in the $SnMo_6S_8$ samples. Although further investigations are needed they explain the causes of this fact, it is probable (see Ref. 44) that it is due to the difference between the elementary pinning forces $f_{p,\,SnMo_6S_8} < f_{p,\,PbMo_6S_8}$ because the basic superconducting parameters of these systems are different.

The pinning-center density can be estimated from the known value of the elastic modulus α by using the formula[4)] (Ref. 32)

$$\alpha=2\sqrt{3}\pi N_p a_f^3 \mu_{\text{eff}}, \qquad (4)$$

where $\mu_{\text{eff}} = 0.15\mu_0 H_{c2}^2 b(1-b)/\varkappa$ is the effective elastic modulus of the vortex lattice in the Labusch theory.[44] Thus, for the sample $PbMo_6S_8$ ($d \approx 0.3$ μm) we obtain $N_p = 1.6 \cdot 10^{20}$ m^{-3}, which corresponds to an average distance $d_p = N_p^{-1/3} \approx 0.19$ μm between pinning centers. For the sample $SnMo_6S_8$ ($d \approx 0.3$ μm) we get $N_p = 0.9 \cdot 10^{20}$ m^{-3} and $d_p = 0.23$ μm. Thus, the values of d_p calculated from Eq. (4) agree well enough with the average grain size $d = 0.3 \pm 0.1$ μm obtained by electron-microscopy. All this offers also evidence that in single-phase $PbMo_6S_8$ and $SnMo_6S_8$ samples the vortex lattice is pinned mainly to grain boundaries.

It is known (see, e.g., Refs. 45 and 46) that there are several mechanisms of pinning to grain boundaries. First is the attachment of the vortex filaments to the grain boundaries of anisotropic superconducting materials, which is due to the differences in the orientations of neighboring crystallites and to the change of the basic superconductor parameters and going through the boundaries. Second, a vortex filament can be pinned to a grain boundary via interaction with the fields of the elastic strains produced in the superconducting material by the dislocations that make up the particular boundary. Finally, pinning to grain boundaries can be due to possible extrusion of impurities or other phases from these boundaries.

In our case it is difficult to single out a definite pinning mechanism on the basis of our results. Interest attaches therefore to the results of Ref. 47, where anisotropy of the upper critical field H_{c2} ($\approx 3\%$) is observed in single crystals of $PbMo_6S_8$ and $SnMo_6S_8$. It is not excluded that the pinning of the vortex lattice by the grain boundaries takes place in the single-phase ternary molybdenum sulfide samples investigated by us precisely because of the anisotropy of the properties of these compounds.

It follows thus from the reported investigations that in bulky single-phase samples of the TMS $PbMo_6S_8$ and $SnMo_6S_8$ the principal pinning centers are apparently the grain boundaries. Since the maximum values of the critical field were obtained in $PbMo_6S_8$ samples with grain size $d \approx 0.3$ μm, it is natural to expect further increase of J_c in samples with even smaller grain size. However, as follows from an analysis of the results, to increase J_c considerably in our samples, particularly in strong magnetic fields, it is necessary to increase the force of vortex pinning to the boundary of each crystallite. This can be achieved, for example, by isolating on the grain boundaries finely dispersed particles of the normal-phase impurity.

In conclusion, the authors thank Academician B. M. Vul for interest in the work, A. I. Rusinov for a helpful discussion and valuable remarks, as well as to E. A. Voĭtekhov for help with electron-microscopy investigations.

[1)]The functions $S(b_0)$, given by the tables of S and b_0, were differentiated with a computer.

[2)]The quantity d_0 is defined as the abscissa of the point of intersection of the horizontal line $F(u_0)/BJ_c = 1$ with the continuation of the initial linear section of the $F(u_0)/BJ_c$ plot.

[3)]Investigation of the reversible responses of vortex lattices in the superconducting alloys Pb + 20% Tl (Ref. 36), Pb + 50% In (Ref. 37), and Pb + Bi (Ref. 30) has shown that $d_0 = \xi/10$. Since $\xi \approx 30$ Å for $PbMo_6S_8$, the same relation between d_0 and ξ holds also in this case.

[4)]Although Eq. (4) was obtained in the limit of a dilute system of pinning centers and neglecting the dependence of α on f_p, it can apparently be used for an approximate estimate of N_p in the investigated $pbMo_6S_8$ and $SnMo_6S_8$ samples.

[1]N. E. Alekseevskiĭ, M. Glinskiĭ, N. M. Dobrovol'skiĭ, and V. I. Tsebro, Pis'ma Zh. Eksp. Teor. Fiz. **23**, 455 (1976) [JETP Lett. **23**, 412 (1975)].
[2]N. E. Alsekseevskiĭ, N. M. Dobrovol'skiĭ, D. Eckert, and V. I. Tsebro, Zh. Eksp. Teor. Fiz. **72**, 1145 (1977) [Sov. Phys. JETP **45**, 599 (1977)].
[3]N. E. Alekseevskiĭ, N. M. Dobrovol'skiĭ, D. Eckert, and V. I. Tsebro, J. Low Temp. Phys. **29**, 565 (1977).
[4]M. Decroux, O. Fisher, and R. Chevrel, Cryogenics **5**, 291 (1978).
[5]N. E. Alekseevskiĭ and A. V. Mitin, Fiz. Met. Metaloved. **50**, 1179 (1980).
[6]V. R. Karasik, E. V. Karyaev, and V. I. Tsebro, *ibid.* **53**, 899 (1982).
[7]N. E. Alekseevskiĭ, A. V. Mitin, and A. V. Knlybov, Zh. Eksp. Teor. Fiz. **82**, 927 (1982) [Sov. Phys. JETP **55**, 543 (1982)].
[8]V. R. Karasik, E. V. Karyaev, M. O. Rikel, and V. I. Tsebro, *ibid.* **83**, 1529 (1982) [**56**, 881 (1982)].
[9]S. A. Alterovitz, U. A. Woolam, L. Kammerdiner, and Huey-Lin Luo, J. Low Temp. Phys. **30**, 797 (1978).
[10]S. A. Alterovitz, J. A. Woolam, L. Kammerdiner, and Huey-Lin Luo, Appl. Phys. Lett. **33**, 264 (1978).
[11]P. Przyslupski, R. Horyn, and B. Gren, J. Low Temp. Phys. **38**, 93 (1980).
[12]K. Hamasaki, T. Inoue, T. Yamashita, T. Komata, and T. Sazaki, Appl. Phys. Lett. **41**, 667 (1982).
[13]T. Luhman and D. Dew-Hughes, J. Appl. Phys. **49**, 936 (1978).
[14]G. Rossel, B. Seeber, and O. Fischer, Phys. St. Sol. (a) **59**, K43 (1980).
[15]B. Seeber, G. Rossel, and O. Fischer, Proc. Int. Conf. on Ternary Superconductor, North Holland, N.Y., 1981.
[16]A. M. Campbell and J. E. Evetts, Critical Currents in Superconductors, Adv. Phys. **21**, 199 (1972).
[17]E. J. Kramer, J. Nucl. Mat. **72**, 5 (1978).
[18]E. J. Kramer, J. Appl. Phys. **49**, 742 (1978).
[19]E. J. Kramer and H. C. Freyhardt, J. Appl. Phys. **51**, 4930 (1980).
[20]T. Matsushita and K. Yamafuji, J. Phys. Soc. Jpn. **50**, 38 (1981).
[21]M. O. Rikel and Z. M. Alekseeva, Izv. AN SSSR, Neorg. Materialy **17**, 2089 (1981).
[22]M. O. Rikel, Z. M. Alekseeva, T. G. Togonidze, V. R. Karasik, and V. I. Tsebro, Kratk. Soobshch. Fiz. (FIAN), No. 12, 3 (1983).
[23]G. T. Wagner and H. C. Freyhardt, J. Phys. Chem. Sol. **43**, 177 (1982).
[24]E. V. Karyaev, Candidate's dissertation, 1982.
[25]A. M. Campbell, J. Phys. **C2**, 1492 (1969).
[26]D. Eckert and A. Handstein, Phys. St. Sol. (a) **37**, 171 (1976).
[27]A. M. Campbell, J. Phys. **C2**, 1492 (1969).
[28]A. M. Campbell, Phil. Mag. **B37**, 169 (1978).
[29]A. M. Campbell, *ibid.* 1191 (1975).
[30]A. M. Campbell, J. Phys. **C4**, 3186 (1971).
[31]E. V. Karyaev, V. M. Zakosarenko, V. R. Karasik, and V. I. Tsebro Preprint No. 269, FIAN SSSR, 1981, p. 38.
[32]T. Matsushita and K. Tamafuji, J. Phys. Soc. Jpn **47**, 1426 (1979).
[33]T. Matsushita and K. J. Yamafuji, *ibid.* **48**, 1885 (1980).
[34]T. Matsushita, Jap. J. Appl. Phys. **20**, 1153 (1981).
[35]T. Matsushita, *ibid.* **20**, 1955 (1981).
[36]T. Matsushita, T. Tanaka, and K. Yamfuji, J. Phys. Soc. Jpn **47**, 1433 (1979).
[37]T. Matsushita and T. Tanaka, *ibid.* **47**, 1433 (1979).
[38]A. I. Larkin, Zh. Eksp. Teor. Fiz. **58**, 1466 (1971) [Sov. Phys. JETP **31**, 784 (1971)].
[39]A. I. Larkin and Yu. N. Ovchinnikov, J. Low Temp. Phys. **34**, 409 (1979).
[40]C. C. Chang, J. B. Mickinnon, and A. C. Rose-Innes, Phys. St. Sol. **36**, 205 (1969).
[41]L. Ya. Vinnikov, V. I. Grigor'ev, and O. V. Zharikov, Zh. Eksp. Teor. Fiz. **71**, 252 (1976) [Sov. Phys. JETP **44**, 130 (1976)].
[42]S. Borka, I. N. Goncharov, D. Friczewski, and I. S. Khukharev, Fiz. Nizk. Temp. **3**, 716 (1977) [Sov. J. Low Temp. Phys. **3**, 347 (1977)].
[43]L. Ya. Vinnikov and O. V. Zharikov, Sol. St. Comm. **28**, 703 (1979).
[44]R. Labusch, Crystal Lattice Defects **1**, 1 (1969).
[45]L. I. Vinnikov, V. G. Glebovskiĭ, I. V. Ermolova, and S. I. Moskvin, Fiz. Met. Metallov. **54**, 268 (1982).
[46]A. Das Gupta, C. C. Koch, D. M. Kroeger, and Y. T. Chou, Adv. Cryog. Eng. **14**, 350 (1978).
[47]N. E. Alekseevskiĭ, V. I. Nizhankovskiĭ, and A. V. Tandut, Abstracts, 22nd All-Union Conf. on Low-Temp. Phys., Kishinev (1982).

Translated by J. G. Adashko